Available online at www.sciencedirect.com

SCIENCE DIRECT®

ELSEVIER

Journal of Nuclear Materials 337–339 (2005) 922–926

journal of nuclear materials

www.elsevier.com/locate/jnucmat

Measurements of chemical erosion of ATJ graphite by low energy D_2^+ impact

F.W. Meyer *, H.F. Krause, L.I. Vergara

Physics Division, Oak Ridge National Laboratory, Oak Ridge, TN 37831-6372, USA

Abstract

We report on initial results of chemical sputtering of ATJ graphite by impact of D_2^+ in the energy range 30–125 eV/amu. A quadrupole mass spectrometer (QMS) in a UHV scattering chamber was used to monitor the partial pressures of species in the atomic mass range 2–60 amu as a function of the D atom dose accumulated on a graphite sample. Based on in situ measurements of cracking patterns and QMS sensitivities using calibrated leaks, sputtering yields are presented for the production of methane and acetylene for sample temperatures of 300 and 800 K, and energies of 30, 45, and 125 eV/amu. At the lowest investigated impact energy, the contribution of CD_4 is found to decrease significantly with increasing temperature, while the contribution of C_2D_2 is virtually unchanged. For an 800K sample temperature, both the CD_4 and C_2D_2 yields increase with increasing impact energy.

PACS: 34.50.Dy; 52.20.Hv; 52.40.Hf; 79.20.−m; 79.20.Rf
Keywords: Carbon-based materials; Chemical erosion; Erosion and deposition; Ion–surface interactions; Sputtering

1. Introduction

One of the critical problems in the development of commercially viable fusion technology is identification of materials for use in plasma facing components (PFCs). Because of their high thermal conductivities, excellent shock resistance, absence of melting, low activation, and low atomic number, carbon-based materials are very attractive candidates for such environments. Different types of graphite or carbon fiber composites (CFCs) are already used in present tokamaks, and CFC tiles (together with some tungsten) are being considered for use in the ITER divertor.

The use of carbon-based materials, however, brings its own set of problems. Oxygen etches carbon very efficiently, forming CO and CO_2 only loosely bound to the carbon surface. At the low plasma temperatures characterizing the divertor environment, chemical erosion of the carbon surface by low energy hydrogen ion impact, leading to the ejection of light hydrocarbon molecules, is significant, and determines in large part the carbon-based-material lifetime. Considering the additional proposed use of Be in PFCs outside the divertor, the potential exists for a complex mixture of materials at the divertor strike points (due to CFC erosion and CFC/W/Be redeposition) that may significantly alter chemical sputtering yields (and thus core impurities and target plate lifetimes). The issue of how these material mixtures

---

[*] Corresponding author. Tel.: +1 865 574 4705; fax: +1 865 574 1118.
E-mail address: meyerfw@ornl.gov (F.W. Meyer).

0022-3115/$ - see front matter © 2004 Elsevier B.V. All rights reserved.
doi:10.1016/j.jnucmat.2004.09.056

affect the chemical sputtering yield from graphite surfaces that have been exposed to high power tokamak operating conditions has remained largely unexplored. Such effects are difficult to explore, at best, in tokamak environments. Laboratory experiments providing fundamental chemical sputtering data in conjunction with theoretical simulations of re- and co-deposition may provide an alternative approach to understanding and assessing the importance of such effects.

For this reason, an experimental research program was started at ORNL to investigate chemical sputtering of graphite surfaces in the limit of very low impact energies. In the present contribution, results are presented for a virgin ATJ graphite surface. In future investigations, the measurements will be extended to ATJ graphite tile samples recently removed from the DIII-D tokamak after exposure to 8 years of tokamak discharges, as well as to virgin HOPG single crystal samples, in order to determine the effects of extensive plasma exposure (i.e., including redeposition and boronization effects) and target structure (i.e., amorphous vs. crystalline, and extent of hydrogen saturation) on chemical sputtering by low energy hydrogen (deuterium) beams.

Laboratory studies of chemical erosion of pyrolytic graphite by low energy (<200 eV) H/D ion impact have been previously reported by Mech et al. [1,2], Davis et al. [3], Balden and Roth [4], and Yamada [5]. Studies on hydrogenated thin films (a-C:H) [6,7] or pyrolytic graphite [8] exposed to thermal hydrogen have been reported as well. Measurements on ATJ graphite samples from DIII-D have been reported by the University of Toronto group in these and previous PSI conference proceedings [9].

2. Experiment

All measurements were performed in a floating potential ultra-high vacuum chamber with base pressures in the 10^{-8} Pa range into which decelerated ion beams from an ECR ion source could be directed, as previously described [10]. A sensitive quadrupole mass spectrometer was installed in the scattering chamber as shown in Fig. 1. The chamber housed, in addition, a time-of-flight analyzer previously used for binary-collision backscattering studies [11]. A grounded baffle between the front end of the QMS and the target sample prevented field penetration from the QMS ionizer section to the region immediately in front of the sample traversed by the low energy ion beams. This baffle also blocked the line-of-sight path from the sample into the analyzer, along which scattered projectiles at higher beam energies could enter and cause unwanted backgrounds in the measured mass spectra. An ATJ (UCAR Carbon Co.) graphite target (same material as used in DIII-D) was used for all the experiments, conditioned prior to mounting by the same procedure employed for the ATJ graphite tiles used in DIII-D. Target temperature variation was achieved by electron-beam-heating, and was monitored by a calibrated infrared (IR) thermal monitor. Sample annealing in excess of 1500 K for about 45 s was performed between measurements in order to reinitialize the sample D inventory. The graphite sample was located 15 mm downstream of the electrostatic deceleration system. Mass selected beams of D_2^+ impacted the sample at normal incidence. The spatial profiles of the incident ion beams were approximately Gaussian in profile with FWHMs in the range 1–2 mm, as determined by a wire scanner that could be inserted in the plane of the target sample. From the beam currents intercepted by the sample and the beam profile measurements, typical beam fluxes of $2–8 \times 10^{15}$ D/cm^2 s were deduced for the present energy range of 30–130 eV/amu. Fluxes in excess of 1×10^{15} D/cm^2 s were obtained down to energies as low as a few eV/amu. Typical vacuum in the test chamber with the beam on was in the low to mid 10^{-7} Pa range.

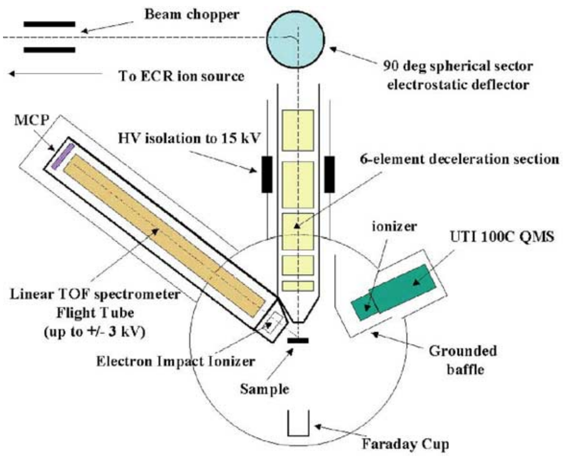

Fig. 1. Schematic diagram of the experimental apparatus.

The experimental approach uses a sensitive quadrupole mass spectrometer which monitors the partial pressures of selected mass species in the range 1–60 amu present in the scattering chamber. A Macintosh-based data acquisition system was used to measure mass distributions at fixed intervals in time, or alternatively, to follow the intensities of selected mass peaks as function of beam exposure times. A strong initial increase with beam dose was observed for all the selected mass peaks, followed by a more gradual increase toward the steady-state peak intensities, where presumably the D concentration in the near-surface region of the graphite sample no longer changed as function of further D irradiation. During each measurement, accumulated beam doses in the $7–9 \times 10^{18}$ D/cm^2 range were reached.

It was crucial to the experimental approach used that all contributions to the chamber pressure other than incident beam related ones be kept constant during the irradiation runs, since the evolution of chemical erosion products during beam irradiation was determined by taking differences between a background pre-irradiation mass spectrum and mass spectra acquired during irradiation at progressively larger accumulated D target doses. In the investigated energy range a significant fraction of the incident D_2^+ beam was re-emitted from the sample, resulting in an increase of the D_2 partial pressure in the scattering chamber during sample irradiation. In the present set-up, reflection of the undissociated but neutralized incident ion is indistinguishable from two D atoms that have recombined in the near surface target region after incident D_2^+ dissociation upon target impact. For all the measurements reported here, the mass 4 peak height observed at sample saturation corresponded to, within the experimental uncertainly of 30%, the D_2 in-flux minus the D contained in the hydrocarbon emission.

In the present article, measurements of mass spectra together with absolute calibrations of the QMS response for deuterium, methane, and acetylene are used to determine chemical sputtering yields of CD_4 and C_2D_2. Because of our limited use of deuterium beams in the test chamber prior to the present investigation, we expect the effect of wall contributions to the quoted yields to be small; however, this will need to be confirmed in future experiments. As described in greater detail below, peaks at masses corresponding to hydrocarbon fragments with D/H substitutions are in fact observed. These, however, were not used in our yield determinations. For fragments whose parentage cannot be ascribed exclusively to fully deuterated hydrocarbons (e.g., mass 24), the quoted sputtering yield values should be considered as upper limits.

3. Selected experimental results

Fig. 2 shows a typical background subtracted mass spectrum for 30 eV/amu D_2^+ normally incident on a 300 K and 800 K ATJ graphite sample after attainment of steady state conditions (i.e., when the intensities of the various observed mass peaks no longer change with increasing D dose). As discussed in the next section, from the known cracking patterns of CD_4 and C_2D_2, it can be deduced that most of the mass 18 peak intensity observed for the 300 K sample temperature originates from the cracking of CD_4 in the ionizer of the QMS, and that the mass 28 peak is mainly due to species such as CO, CND, and/or N_2, i.e., contains only a small contribution from C_2D_2. The small peaks at mass 40 are due to Ar. This species most likely arises due to interaction of reflected energetic D projectiles with trace amounts of Ar remaining on the chamber walls from earlier sputtering cycles. The ATJ sample itself was not sputter cleaned and should therefore not contain Ar.

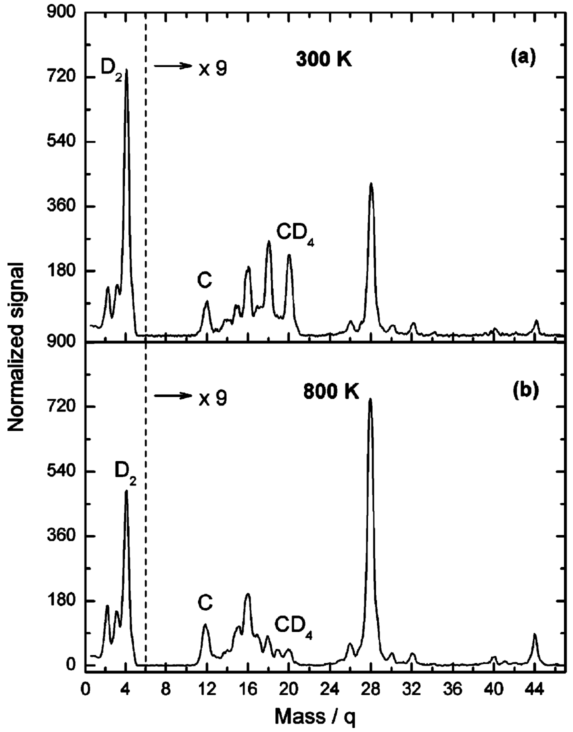

Fig. 2. Background-subtracted mass spectra obtained after saturation of all mass peaks. intensities for (a) room temperature and (b) 800 K ATJ graphite irradiated by normally incident 30 eV/amu D_2^+. The normalized signal corresponds to mass peak amplitude divided by the incident beam current.

The mass spectrum acquired at the 800 K sample temperature shows a significantly reduced CD_4 intensity in comparison to the room temperature sample case and an increase in mass 44 intensity, ascribed to CO_2. The intensities of mass peaks in the 12–19 amu range at 800 K arise mainly from cracking of CO, CND, N_2, and CO_2, and wall contributions, as discussed below.

To illustrate the primary beam energy dependence of the chemical erosion for an elevated sample temperature of 800 K, Fig. 3 shows the change of the measured mass spectra with increasing D_2^+ impact energy: most dramatic is the increase in CD_4 production at the highest beam energy of 125 eV/amu, with more modest increases in the heavier hydrocarbons evidenced as well.

4. Discussion

In order to interpret the observed mass spectra, in situ measurements of cracking patterns and absolute QMS response were performed for D_2, CH_4, and C_2H_2

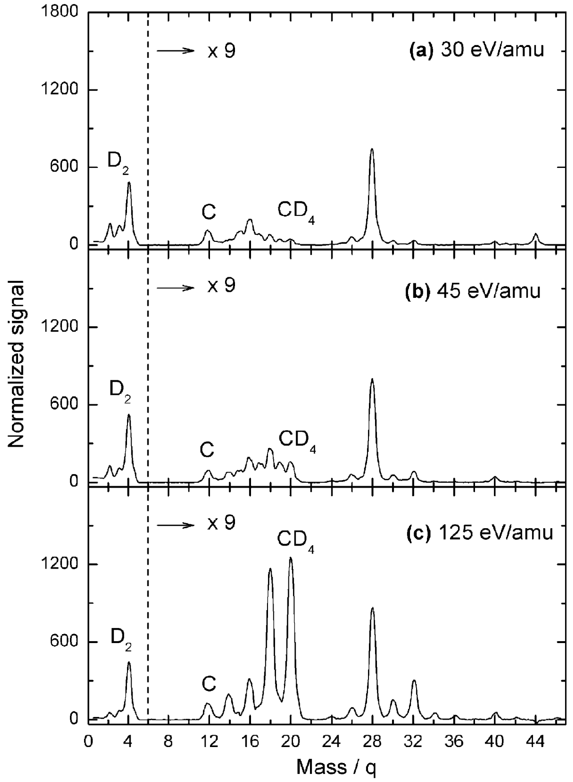

Fig. 3. Background-subtracted mass spectra obtained at three different beam energies for an 800 K ATJ graphite sample, irradiated until saturation was reached; (a) 30 eV/amu, (b) 45 eV/amu, and (c) 125 eV/amu.

using UHV-compatible calibrated leaks. The measured cracking patterns were found to be in good agreement with tabulated values for this instrument [12]. With the instrument response thus verified, and assuming that the light hydrocarbon fragmentation is independent of H/D isotopic make-up, the cracking patterns of CD_4, C_2D_2, C_2D_4, C_2D_6, C_3D_6, and C_3D_8 and the intensity distributions of the observed mass spectra were used in selecting peaks representative of CD_4 and C_2D_2 that had minimum interference with other hydrocarbon species. On this basis, the peaks at masses 20 and 24 were used in determining the chemical sputter yields for CD_4 and C_2D_2, respectively. The mass 20 peak was found to be essentially free from interferences, while the mass 24 peak required a less than 25% intensity correction due to heavier hydrocarbon species. These two (corrected) peak intensities and the mass 4 peak, together with the absolute QMS response calibration, were used to determine the sputter yields for CD_4 and C_2D_2 shown in Table 1. In correcting the incident beam currents for secondary electron emission, γ values of 0.05, 0.1, and 0.2 were assumed for the three investigated energies, in order of increasing energy.

Table 1
Summary of chemical yields of CD_4 and C_2D_2 for D_2^+ incident on ATJ graphite for different incident energies and sample temperatures; the quoted results are steady-state values reached after extended beam exposure

Sample temperature (K)	Energy (eV/amu)	CD_4	C_2D_2
300	30	6.8×10^{-3}	3.5×10^{-3}
800	30	1.4×10^{-3}	4.2×10^{-3}
800	45	5.1×10^{-3}	8.0×10^{-3}
800	125	4.3×10^{-2}	1.5×10^{-2}

Units are CD_4, or C_2D_2 per incident D, respectively. Total estimated uncertainties are 30%.

Although the most prominent of all the observed peaks, the peak at mass 28 was eliminated as a possible representative of C_2D_2, because of significant interferences from heavier hydrocarbons, and, more importantly, from other species (i.e., CO, CND, and N_2). The use of mass peaks below 20 amu was similarly avoided, because of likely contributions from the cracking of CO, CO_2, and possibly CND, and from hydrocarbons adsorbed on the chamber walls. Any H in the bulk of the ATJ sample has been presumably thermally desorbed during flash annealing cycles performed both prior to and during the present measurements. The chamber walls, on the other hand, have not been outgassed at temperatures exceeding 200 °C, and so can still have significant inventories of H and H-based light hydrocarbons. For example, the spectra in Figs. 2(b) and 3(b) show the mass 19 signal to be as large as the mass 20 signal, suggesting the production of mixed isotope hydrocarbons, presumably in wall collisions. Thus, in particular, the unaccounted for mass 18 and 19 intensities remaining after accounting for hydrocarbon cracking could be due in large part to CD_2H_2 and CD_3H generated at the chamber walls. This general complication of partial pressure measurements in the determination of chemical sputtering products due to 'wall' collision contributions has been noted by Mech et al. [1]. In the present measurements, by concentrating on mass peaks whose intensities are fully accounted for by cracking of completely deuterated erosion products, we believe such effects are largely eliminated, since our UHV chamber has only seen limited exposure to D_2.

It is noted that our temperature dependence of CD_4 production observed at the lowest investigated energy of 30 eV/amu contrasts with published energetic ion impact results for pyrolytic graphite [1] at this energy. Our observed temperature dependence, showing an almost factor of three decrease of CD_4 production as the sample temperature is increased from room temperature to 800 K, is similar to that reported for thermal H impact, also on pyrolytic graphite [8]. However, unlike the present measurements, no acetylene production was observed in the latter work below 1000 K. Interestingly, as will be discussed in greater detail elsewhere [13], at higher energies (e.g., 125 eV/amu), we observe that CD_4 production *increases* with increasing sample temperature in the range 300–800 K, a trend more in line with existing energetic ion impact results [1–4]. Also, more in line with published energetic ion impact results is our observed sample temperature dependence for C_2D_2 production at 30 eV/amu, as well as the ion impact energy dependence at a sample temperature of 800 K.

5. Conclusion

Chemical sputtering yields of CD_4 and C_2D_2 due to 30–125 eV/amu D_2^+ impact at normal incidence on ATJ graphite have been measured for a sample temperature of 800 K, and for a 300 K sample temperature at 30 eV/amu. At the latter energy the CD_4 yield at 300 K exceeds that at 800 K by almost a factor of 5. The CD_4 yield from the 800 K sample increases steeply with increasing energy, reaching a value of almost 5% per incoming D at 125 eV/amu. In contrast, the C_2D_2 yield increases as the sample temperature is increased from 300 K to 800 K at the lowest energy, as well as with increasing ion impact energy, reaching a value of almost 2% per incoming D for an 800 K sample temperature and an impact energy of 125 eV/amu.

Acknowledgments

We are indebted to S.H. Overbury for making available the QMS and sample holder used in the present measurements, and to J.W. Davis, A.A. Haasz and W. Jacob for valuable discussions and suggestions. This research was sponsored by the Office of Fusion Energy Sciences and the Office of Basic Energy Sciences of the US Department of Energy under contract No. DE-AC05-00OR22725 with UT-Battelle, LLC. L.I.V. was appointed through the ORNL Postdoctoral Research Associates Program administered jointly by Oak Ridge Institute of Science and Education and Oak Ridge National Laboratory.

References

[1] B.V. Mech, A.A. Haasz, J.W. Davis, J. Nucl. Mater. 255 (1998) 153;
B.V. Mech, PhD. thesis, University of Toronto, 1997.
[2] B.V. Mech, A.A. Haasz, J.W. Davis, J. Nucl. Mater. 241–243 (1997) 1147.
[3] J.W. Davis, A.A. Haasz, P.C. Stangeby, J. Nucl. Mater. 155–157 (1988) 234.
[4] M. Balden, J. Roth, J. Nucl. Mater. 280 (2000) 39.
[5] R. Yamada, J. Nucl. Mater. 145–147 (1987) 359.
[6] E. Vietzke, K. Flaskamp, V. Phillips, G. Esser, P. Wienhold, J. Winter, J. Nucl. Mater. 145–147 (1987) 443.
[7] T. Zecho, B.D. Brandner, J. Biener, J. Küppers, J. Phys. Chem. B 105 (2001) 6194.
[8] M. Baloch, D.R. Olander, J. Chem. Phys. 63 (1975) 4772.
[9] G.M. Wright, A.A. Haasz, J.W. Davis, R.G. Macaulay-Newcombe, these Proceedings, doi:10.1016/j.jnucmat.2004.10.009;
J.W. Davis, P.B. Wright, R.G. Macauley-Newcombe, A.A. Haasz, C.G. Hamilton, J. Nucl. Mater. 290–293 (2001) 66;
P.B. Wright, J.W. Davis, R.G. Macaulay-Newcombe, C.G. Hamilton, A.A. Haasz, J. Nucl. Mater. 158–162 (2003) 158.
[10] V.A. Morozov, F.W. Meyer, Rev. Sci. Instrum. 70 (1999) 4515.
[11] V.A. Morozov, F.W. Meyer, Phys. Rev. Lett. 86 (2001) 736.
[12] UTI 100C Operating Manual.
[13] L.I. Vergara, H.F. Krause, F.W. Meyer, J. Chem. Phys., submitted for publication.